

Article

Assessment of the Binding of Protons, Al and Fe to Biochar at Different pH Values and Soluble Metal Concentrations

Tan Dang ^{1,*}, Petra Marschner ², Rob Fitzpatrick ¹ and Luke M. Mosley ¹

¹ Acid Sulfate Soils Centre, The University of Adelaide, Adelaide, SA 5005, Australia; Rob.Fitzpatrick@csiro.au (R.F.); Luke.Mosley@adelaide.edu.au (L.M.M.)

² School of Agriculture, Food and Wine, The University of Adelaide, Adelaide, SA 5005, Australia; petra.marschner@adelaide.edu.au

* Correspondence: Tan.Dang@adelaide.edu.au

Received: 12 December 2017; Accepted: 7 January 2018; Published: 10 January 2018

Abstract: Biochar can retain large amounts of protons and metals in the drainage water from acid sulfate soils and mine sites. Metal sorption can, however, be influenced by many factors, such as pH and metal composition. This study investigated proton, Al, and Fe retention capacity of eucalyptus biochar (1% *w/v*) at different pH and metal concentrations. In the absence of metals, the biochar had a high proton binding capacity, (up to 0.035 mmol of H⁺), whereas its capacity to retain hydroxide ions was limited. A batch experiment was carried out at pH 4 and pH 7 with 10⁻⁶, 10⁻⁵, 10⁻⁴, 10⁻³, and 10⁻² M of added Fe or Al. Added metals precipitated considerably prior to addition of the biochar except that Al remained highly soluble at pH 4. The biochar had a high retention capacity for Al and Fe; at high (>1 mM) concentrations, over 80% of soluble metals were retained. Metal competition for binding sites of both Al and Fe at different ratios was investigated, but increasing concentrations of one metal did not reduce retention of the other. The results confirmed that biochar has high metal binding capacity under both acidic and neutral conditions.

Keywords: biochar; acid sulfate soil; proton; metal binding

1. Introduction

Upon rewetting due to rainfall or flooding, sulfuric (pH < 4) material in acid sulfate soils (ASS) can release large amounts of acidity and soluble metals (particularly Al and Fe) to ground and surface water [1,2]. Some ASS have been drained for over hundred years and are still discharging acidity into streams or waterways [3]. White, et al. [4] predicted that ASS in floodplains containing iron sulfide rich materials may be continuously oxidised for thousands of years. It is estimated that one tonne of sulfide produces approximately one and a half tonnes of sulfuric acid [3]. ASS in floodplains of the Tweed river (New South Wales, Australia) discharged approximately 110 kg of sulfuric acid per hectare in a few days of rain [5]. Drainage water seeping from sulfuric material (pH < 4) in ASS also contains high amounts of metals that are released due to the low pH. Concentrations of Al, As, Cd, Co, Cr, Cu, Ni, Pb, V, and Zn in pore and drainage water have been shown to exceed Australian Water Quality Guidelines [6], up to 100 fold [1,7].

We showed previously that organic materials, such as plant residues, composts, and biochar retained large amounts of protons and Al and Fe from ASS drainage water and released less than 1% of that retained when subsequently leached with pure water [8,9]. Among the materials that were tested, retention was greater in biochars and composts than in plant residues. Biochar has received considerable interest as a low cost and sustainable biosorbent to remove metal contamination such as As, Cd, Pb, Zn from waste water or acid mine drainage water [10–15]. Metal adsorption efficiency

varied, however, and is affected by factors, such as functional groups, surface area, and environmental conditions [10,16,17]. Metal retention on organic materials is strongly pH dependent [18,19]. As pH increases, there is less competition for cation binding sites with protons [18]. Additionally, dissolved metals may precipitate as pH increases (e.g., [20]).

Acidity of ASS drainage water varies over time [21–25]. It is well-known that pH plays an important role in metal speciation, solubility, and complexation. For example, ferrous iron Fe(II) is often dominant in acidic reducing environments [26,27]. Under acidic oxidising conditions, ferric species [Fe(III)] in the form of iron oxyhydroxide (e.g., Schwertmannite, Jarosite) minerals are precipitated [26,28]. The effect of pH on aluminium speciation is quite complex [29,30]. At pH above 5, aluminium is predominantly present as mononuclear species AlOH_2^+ , $\text{Al}(\text{OH})_2^+$, $\text{Al}(\text{OH})_3$, and $\text{Al}(\text{OH})_4^-$, or forms soluble complexes with e.g., sulfate or fluoride [29]. Between pH 3 and 5, such as commonly found in areas impacted by sulfuric material in ASS, Al^{3+} species are dominant [30]. At pH 7, insoluble $\text{Al}(\text{OH})_3$ or polynuclear aluminium species are formed [29].

pH is likely to influence metal binding to biochar, through its effect on cation exchange capacity, surface complexation, metal solubilisation, and precipitation. More systematic studies are needed to better understand proton, Al and Fe binding to biochar to optimise its use in semipermeable barriers for ASS drainage water. The main objective of this study was to evaluate the proton and Al and Fe retention capacity of eucalyptus biochar produced at 550 °C that had showed high Al and Fe retention in our earlier studies (Dang et al. 2016). Proton sorption to biochar was tested by acid-base titration in the absence of metals. A series of batch experiments was conducted at either pH 4 or 7 to investigate individual binding of Al and Fe to biochar. Further, a competition experiment with Al and Fe was conducted at pH 7.

2. Materials and Methods

2.1. Experimental Design

Eucalyptus biochar used in this study was produced by pyrolysis of raw plant material in a low-oxygen environment at 550 °C and ground and sieved to less than 0.5 mm. The biochar then was washed four times with reverse osmosis (RO) water at a 1:10 ratio (*w/v*) to remove salts until the conductivity of the leachate was low and stable ($\text{EC} < 0.05 \text{ dS m}^{-1}$). The washing protocol was amended from a pre-treatment method for measuring exchangeable cations [31]. The biochar was then dried at 40 °C.

For the experiment of proton binding to biochar, titration procedures were amended from the pH buffer capacity measurement protocol developed by Aitken and Moody [32]. The biochar (0.25 g) was added to 20 mL of 0.1 M KNO_3 background pH electrolyte solution. The solutions were titrated to pH 3, 3.5, 4, 4.5, 5, 5.5, 6, 6.5, 7, 7.5, 8, 9, and 10 with standardized 0.04 M HNO_3/KOH . There were three replicates of each pH solution. Then, 0.1 M KNO_3 solution was added to reach a final volume of 25 mL. The suspensions were equilibrated for 24 h on an end-over shaker at room temperature followed by further addition of standardized 0.04 M HNO_3/KOH until the desired pH was reached. The volume of standardized 0.04 M HNO_3/KOH added was recorded.

For the experiments of single metal binding to biochar, Al and Fe adsorption isotherms were determined at constant pH 4 or pH 7 in a batch approach in accordance with Weber, et al. [33]. These two pH values were chosen because we assumed that binding capacity of the biochar would be smaller at pH 4 than pH 7 due to protonation of potential metal binding sites. Biochar (0.25 g) was added to a 50 mL tube containing 20 mL of 0.1 M KNO_3 background pH electrolyte solution. Different amounts of $\text{Al}(\text{NO}_3)_3$ and $\text{Fe}(\text{NO}_3)_3$ stock solutions were added to the tubes to give metal concentrations of 10^{-6} , 10^{-5} , 10^{-4} , 10^{-3} , and 10^{-2} M. The control was 0.25 g biochar in 25 mL of 0.1 M KNO_3 solution. The pH of the suspensions was adjusted to 4 or 7 by standardised 0.04 M HNO_3 or KOH . The suspensions were equilibrated for 24 h on a horizontal shaker after which the pH was again adjusted to either 4 or 7. After another 24 h on the shaker, the pH was again re-adjusted to the desired

pH if necessary (total equilibration time 48 h). Then, 0.1 M KNO₃ solution was added to reach the final volume of 25 mL. Concentrations of soluble Fe and Al were measured, as described below. There were three replicates per metal and pH combination.

For the Al/Fe competition experiment the pH was adjusted to 7, as described above. Iron concentrations (added as Fe(NO₃)₃) of 10×10^{-3} , 5×10^{-3} , and 1×10^{-3} M) were combined with Al concentrations (added as Al(NO₃)₃) of 10×10^{-3} , 5×10^{-3} , and 1×10^{-3} M). There were three replicates per combination.

In addition, to test the influence of metal precipitation on the concentration of soluble Al and Fe at pH 4 and 7, soluble metal (<0.025 µm filtered) concentrations in the absence of biochar were measured after 48 h equilibration using the same metal concentrations and procedures described above.

2.2. Analyses

The pH of the biochar was measured in RO water at a 1:1 ratio (*w/w*). Total organic C and total N of the biochar were measured by dry combustion using a LECO Trumac CN analyser (LECO Corporation, Saint Joseph, MI, USA).

Acid neutralising capacity (ANC) expressed as CaCO₃ equivalent was determined by the rapid titration method, as described in Ahern, et al. [34]. Briefly, 1 g of finely ground biochar was placed into a 250 mL flask with 50 mL of deionised water and 25 mL of standardised 0.1 M HCl. The suspensions were boiled on a hotplate for 2 min and then allowed to cool to room temperature. The unreacted acid in the flask was titrated with standardised 0.1 M NaOH to pH 7.

Surface area was analysed by a nitrogen gas adsorption method and calculated, as described by Brunauer, et al. [35]. The biochar was degassed overnight at a vacuum of 10^{-5} kPa prior to measuring nitrogen adsorption. Biochar was degassed at 200 °C. Nitrogen gas adsorption was measured at 77K using a Belsorp-max gas adsorption apparatus. Ultra high purity (>99.999%) helium and nitrogen were used for dead space measurements and adsorption experiments, respectively.

Cation exchange capacity (CEC) was determined after Rayment and Lysons [31]. The biochar was extracted with 0.1 M NH₄Cl at a 1:30 *w/w* ratio in an end-over-end shaker for 1 h. The extracts were centrifuged at 3000 rpm for 10 min, the supernatant filtered through Whatman #42 filter paper. The solution was analysed by inductively coupled plasma optical emission spectroscopy (ICP-OES, Agilent, Mulgrave, Australia).

Acid extractable Al and Fe in the biochar were determined after aquaregia (1:3 concentrated HNO₃:HCl) acid dissolution [36]. The extracts were filtered through Whatman #42 filter paper and were analysed for Al and Fe by ICP-OES.

Chemical groups of biochar were measured by solid-state ¹³C nuclear magnetic resonance (NMR) spectroscopy, as described in McBeath, et al. [37]. ¹³C NMR detects carbon atoms and groups such as alkenes, aldehydes through the specific shift in magnetic resonance of each structure.

The amount of standardised HNO₃ and KOH added to the solution containing 1% (*w/v*) of eucalyptus biochar were expressed as mmol of acid and base to obtain the titration curve.

The solutions from the precipitation experiment (no biochar present) were filtered onto 0.025 µm nitrocellulose membrane filters, the soluble Al and Fe in the filtrates were then measured by ICP-MS (Agilent, Mulgrave, Australia). The soluble metal concentrations were expressed as µg per tube.

The solutions of single metal binding or metal binding competition experiments were centrifuged at 4000 rpm for 30 min. The supernatants were then removed and filtered through 0.025 µm nitrocellulose membrane filters before measuring metal concentrations by ICP-MS. Binding of Al and Fe to biochar (µg metal/g biochar) was calculated, as follows: [added soluble metal per tube (µg) – (concentration of metal in filtrate (µg/L) × volume (L) of filtrate solution per tube)]/amount of biochar (g) per tube.

Data was analysed by one way ANOVA. Differences between means were compared by Duncan analysis ($p \leq 0.05$) using GenStat 15th edition (GenStat 2013).

3. Results

The properties of eucalyptus biochar produced at 550 °C are presented in Table 1. The biochar had a pH of 7.5, a high organic C concentration (552 mg g⁻¹), low total N concentration (5.6 mg g⁻¹) and therefore high C/N ratio (approx. 100). The ANC (3.8% CaCO₃), CEC (39 cmol kg⁻¹) and surface area (2.5 m² g⁻¹) of the biochar were moderate compared to other biochars (for details see Dang et al. [8]), whilst the extractable Al and Fe concentrations were high. The dominant functional groups were Alkyl, Aryl, and O-Aryl C.

Table 1. Properties of eucalyptus biochar 550 °C.

	pH _w	7.5
TOC	mg g ⁻¹	551.6
Total N	mg g ⁻¹	5.6
C/N		98
ANC	% CaCO ₃	3.8
CEC	cmol(+) kg ⁻¹	39.3
Surface area	m ² g ⁻¹	2.5
Acid extractable Al	mg g ⁻¹	3.8
Acid extractable Fe	mg g ⁻¹	19.8
Chemical functional groups	% C detected	
Alkyl		10.3
N-Alkyl/Methoxyl		3.1
O-Alkyl		4.5
Di-O-Alkyl		3.6
Aryl		57.5
O-Aryl		13.6
Amide/Carboxyl		4.3
Ketone		3.2

The biochar had a high proton binding capacity, whereas its capacity to bind OH⁻ was limited as pH increased rapidly when base was added (Figure 1).

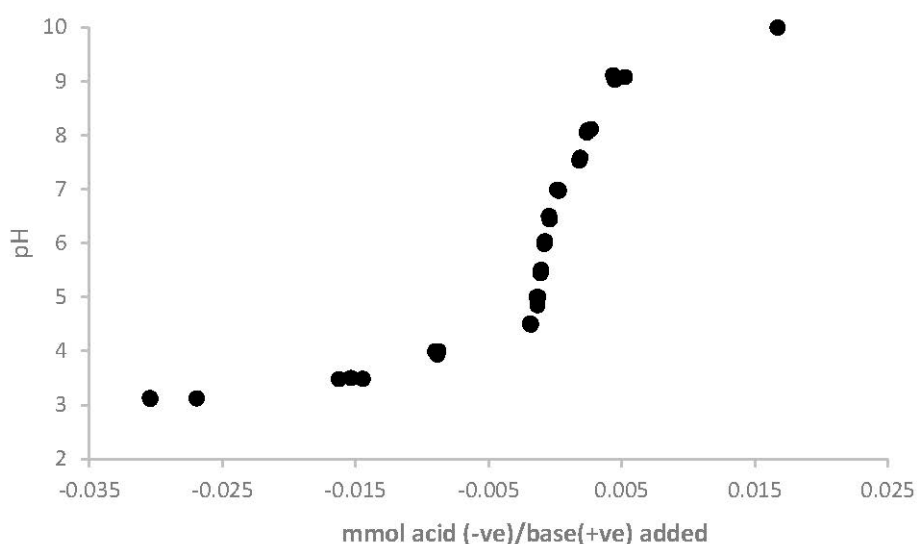


Figure 1. Effect of addition of acid(−ve)/base(+ve) to 1% (*w/v*) mallee biochar on pH.

In the absence of biochar at pH 4, all of the added Al remained soluble up to an Al concentration of 0.1 mM. At higher concentrations, about two-thirds of the added Al remained soluble (Table 2). At pH 7 on the other hand, only about one third of the added Al was soluble up to Al concentrations

of 0.1 mM. At higher concentrations, less than 10% of the added Al was soluble. Less than 1% of added Fe remained soluble at pH 4 and pH 7 except at the lowest addition rate (Table 3). Soluble Fe concentrations were lower at pH 7 than pH 4.

Table 2. Soluble Al in solution (no biochar present) at different concentrations after adjustment to pH 4 and pH 7.

Added Al		Amount of Soluble Al after Adjusted pH (μg per tube)	
(mM)	(μg per tube)	pH 4	pH 7
0.001	0.7	0.7	0.7
0.01	6.7	6.7	2.3
0.1	67.5	67.5	15.9
1	674.5	562.6	21.3
5	3372.5	2177.8	29.8
10	6745.0	4302.5	36.7

Table 3. Soluble Fe in solution (no biochar present) at different concentrations after adjustment to pH 4 and pH 7.

Added Fe		Amount of Soluble Fe after Adjusted pH (μg per tube)	
(mM)	(μg per tube)	pH 4	pH 7
0.001	1.4	1.3	1.3
0.01	14.0	2.1	1.6
0.1	139.6	9.1	6.7
1	1396.3	43.5	47.7
5	6981.3	229.0	339.9
10	13,962.5	685.2	415.8

With biochar at pH 4 and 7 and the three highest Al addition rates (270–17,210 μg Al/g biochar), more than 90% of added soluble Al was bound to the biochar. At pH 7 and lower Al addition rates (3–27 μg Al/g biochar), between 60 and 75% of added soluble Al was bound to the biochar. At pH 4, 50% of the 27 μg Al/g biochar was bound, whereas no binding was measured in the 3 μg Al/g biochar treatment. Because of the release of native Al from the biochar, no binding could be detected at the lowest Al addition (0.001 mM) rate at pH 4 (Table 4).

At higher Fe addition rates, 83–91% of added soluble Fe was bound to the biochar at pH 4 and 7. At pH 7 and 5–6 μg Fe/g biochar addition, about 70% of added soluble Fe was bound to biochar. At higher Fe addition rates (27–1663 μg Fe/g biochar), 87–99% of added soluble Fe was bound. No Fe binding was detected at pH 4 at the three lower addition rates due to release of native Fe (Table 5).

In the Fe/Al competition experiment, 99% of the added soluble Fe was bound to the biochar (Table 6). Iron reduced the percentage of bound Al only at the lowest Al addition rate (85 μg soluble Al g^{-1}), combined with the lowest Fe addition rate (191 μg soluble Fe g^{-1}). At the higher Al addition rates, more than 95% of added soluble Al was bound to the biochar.

Table 4. Al binding to biochar at pH 4 and pH 7.

Soluble Added ($\mu\text{g}/\text{g}$)	pH 4		Soluble Added ($\mu\text{g}/\text{g}$)	pH 7	
	Binding ($\mu\text{g}/\text{g}$)	Binding (%)		Binding ($\mu\text{g}/\text{g}$)	Binding (%)
0	−20	0	0	−1	0
3	−9	0	3	2	60.5
27	14	51.0	9	7	74.7
270	243	90.1	64	61	95.9
2250	2096	93.1	85	80	93.9
17,210	16,990	98.7	147	140	95.4

Table 5. Fe binding to biochar at pH 4 and pH 7.

Soluble Added ($\mu\text{g/g}$)	pH 4		pH 7		
	Binding ($\mu\text{g/g}$)	Binding (%)	Soluble Added ($\mu\text{g/g}$)	Binding ($\mu\text{g/g}$)	Binding (%)
0	−18	0	0	−1	0
5	−13	0	5	4	74.6
8	−13	0	6	4	64.2
37	31	83.7	27	25	93.3
174	153	88.0	191	189	98.8
2741	2489	90.8	1663	1438	86.5

Table 6. Al and Fe binding to biochar at pH 7 in mixtures of different metal concentrations.

Soluble Added		Binding			
		Al ($\mu\text{g/g}$)	%	Fe ($\mu\text{g/g}$)	%
Fe ($\mu\text{g/g}$)	Al ($\mu\text{g/g}$)				
191	85	82.5	89.5	190.3	99.7
	119	113.1	96.7	188.3	98.7
	147	140.7	99.5	188.4	98.7
1360	85	83.2	97.8	1358.2	99.9
	119	113.4	95.3	1356.2	99.8
	147	120.6	97.5	1355.5	99.7
1663	85	84.9	95.7	1662.6	100
	119	115.4	94.8	1660.7	99.9
	147	131.5	96.8	1658.8	99.7

4. Discussion

This study showed that the eucalyptus biochar had a high proton, Al and Fe binding capacity. Biochar can contain humification products (fulvic acid- and humic acid-like materials), which contribute to their proton binding capacity [38,39]. Humic acids are important components of decomposed organic matter which have high proton affinity and metal binding [39]. Models (e.g., NICA-Donnan) of proton and metal binding to carboxylic acid functional groups (and phenolic groups at higher pH) on humic acids [39,40] suggest that metal binding should greatly reduce at pH 4. But, the biochar-metal binding behaviour in this study did not show a strong pH dependence. This was unexpected based on a prior assumption of a lack of negatively charged binding sites found on humic acid at pH 4 [18,19]. However, the reverse was true; more Al and Fe were bound at pH 4 than at pH 7, with higher soluble metal concentrations present in added solution at the lower pH. These results suggest that other functional groups and/or properties contributed more to proton and metal binding. Carboxylic acid groups comprised only a minor proportion (4.3%) of the eucalyptus biochar functional groups based on our ^{13}C NMR analysis (Table 1). Our results suggest the models developed for metal binding to natural organic matter in water and soils are not readily applicable to biochar. Other potential binding mechanisms for metals include ion exchange, surface complexation, electrostatic attraction, or physical adsorption [18,41]. It is clearly an advantage, however, if biochar can bind metals under acidic conditions, as these are the conditions in the drainage water from acid sulfate soils and mine sites. The lack of competition between Fe and Al when both metals were added may also be due to their being sufficient binding sites for both metals and protons at the concentrations used in the experiment. Alternatively, there may be different binding sites for these two metals. Again, these findings appear to differ from those found for the NICA-Donnan model of metal binding to organic matter [42]. There was some release of native Al and Fe from the biochar, which resulted in no apparent binding at low Al and Fe addition rates.

Speciation of Al and Fe in solution is complex and controlled by pH [29,30]. In this study, a large proportion of added Al and Fe precipitated prior to adding biochar, even at pH 4, possibly due to hydrolysing and oxidizing conditions during shaking of the suspension. However, at low pH (pH 4) and highest addition rate (10 mM), residual soluble Al (172 mg L^{-1}) and Fe (28 mg L^{-1}) concentrations were higher than have been found in drainage water from oxidised ASS (Al: 2 mg L^{-1} ; Fe: 28 mg L^{-1}) [26]. As 90% or more of the dissolved Al and Fe were bound, even at high concentrations, the maximum binding capacity of biochar is greater than $17,000 \text{ } \mu\text{g Al}$ and $2700 \text{ } \mu\text{g Fe}$ per g of biochar. Based on the above drainage ASS concentrations, this equates to each tonne of biochar being able to treat Al and Fe in approximately 8.5 mL and 0.1 mL of drainage water, respectively. Given that dissolved Al is much more toxic to aquatic organisms than Fe, which is considered non-toxic [6], the reduction in retention capacity for Fe is not of major concern. However, the hydrolysis of dissolved Fe can consume protons and potentially acidify water downstream [43], so Fe removal capacity is still beneficial. Once acid was applied to the biochar, solid phase carbonate in the biochar may have dissolved, increased pH (due to formation of HCO_3^-), and induced metal precipitation within the solution and to the biochar. The eucalyptus biochar had 4% CaCO_3 (Table 1), therefore some protons will also be neutralised by carbonates [44,45], although we adjusted to a set pH in the experiments.

In summary, the results suggest that biochar has potential for metal and proton removal over a wide range of soluble metal concentrations, as they may occur in drainage channels of acidic ASS, which is in agreement with our previous studies [8,9]. Pilot scale field trials are required to confirm this. Potential limitations of using biochar in drainage channels could be saturation of the binding capacity and disposal of the biochar after use. Further laboratory-based investigations and modelling of metal-binding sites on biochar would also be beneficial.

Acknowledgments: Tan Dang is grateful to the Vietnam International Education Development (VIED) for providing the postgraduate scholarship. We thank Lynne Macdonald for providing the biochars, Seyed Hadi Madani for analysing surface area, Ron Smernik for analysing chemical functional group by NMR analysis and Bogumila Tomczak for measuring Al and Fe by ICP-OES.

Author Contributions: Tan Dang carried out the experiment and drafted the manuscript under the supervision of Petra Marschner, Rob Fitzpatrick and Luke M. Mosley. Petra Marschner and Luke M. Mosley conceived and designed the experiment. Petra Marschner, Rob Fitzpatrick and Luke M. Mosley helped to analyse the data revised manuscript. All authors have read and approved the final manuscript.

Conflicts of Interest: The authors declare no conflict of interest.

References

1. Simpson, S.; Fitzpatrick, R.; Shand, P.; Angel, B.; Spadaro, D.; Merry, R.; Thomas, M. Chapter 3: Acid and Metal Mobilisation Following Rewetting of Acid Sulfate Soils from the River Murray, South Australia: A Rapid Laboratory Method. In *Inland Acid Sulfate Soil Systems across Australia*; Fitzpatrick, R., Shand, P., Eds.; CRC LEME: Perth, Australia, 2008; pp. 90–97.
2. Cook, F.J.; Hicks, W.; Gardner, E.A.; Carlin, G.D.; Froggatt, D.W. Export of Acidity in Drainage Water from Acid Sulphate Soils. *Mar. Pollut. Bull.* **2000**, *41*, 319–326. [[CrossRef](#)]
3. Sammut, J.; Lines-Kelly, R. *An Introduction to Acid Sulphate Soils*; Natural Heritage Trust: Sydney, Australia, 2000.
4. White, I.; Melville, M.D.; Wilson, B.P.; Sammut, J. Reducing acidic discharges from coastal wetlands in eastern Australia. *Wetl. Ecol. Manag.* **1997**, *5*, 55–72. [[CrossRef](#)]
5. Macdonald, B.C.T.; White, I.; Åström, M.E.; Keene, A.F.; Melville, M.D.; Reynolds, J.K. Discharge of weathering products from acid sulfate soils after a rainfall event, Tweed River, eastern Australia. *Appl. Geochem.* **2007**, *22*, 2695–2705. [[CrossRef](#)]
6. Australian and New Zealand Environment and Conservation Council (ANZECC). *Australian and New Zealand Guidelines for Fresh and Marine Water Quality*; Australian and New Zealand Environment and Conservation Council and Agriculture and Resource Management Council of Australia and New Zealand: Canberra, Australia, 2000.
7. Hicks, W.; Fitzpatrick, R.; Bowman, G. Managing coastal acid sulfate soils: The East Trinity example. In *Advances in Regolith*; Roach, I.C., Ed.; CRC LEME Regional: Bentley, WA, USA, 2003; pp. 174–177.

8. Dang, T.; Mosley, L.M.; Fitzpatrick, R.; Marschner, P. Organic materials retain high proportion of protons, iron and aluminium from acid sulphate soil drainage water with little subsequent release. *Environ. Sci. Pollut. Res.* **2016**, *23*, 23582–23592. [[CrossRef](#)] [[PubMed](#)]
9. Dang, T.; Mosley, L.M.; Fitzpatrick, R.; Marschner, P. Addition of organic material to sulfuric soil can reduce leaching of protons, iron and aluminium. *Geoderma* **2016**, *271*, 63–70. [[CrossRef](#)]
10. Lu, H.; Zhang, W.; Yang, Y.; Huang, X.; Wang, S.; Qiu, R. Relative distribution of Pb²⁺ sorption mechanisms by sludge-derived biochar. *Water Res.* **2012**, *46*, 854–862. [[CrossRef](#)] [[PubMed](#)]
11. Trakal, L.; Bingöl, D.; Pohořelý, M.; Hruška, M.; Komárek, M. Geochemical and spectroscopic investigations of Cd and Pb sorption mechanisms on contrasting biochars: Engineering implications. *Bioresour. Technol.* **2014**, *171*, 442–451. [[CrossRef](#)] [[PubMed](#)]
12. Elaigwu, S.E.; Rocher, V.; Kyriakou, G.; Greenway, G.M. Removal of Pb²⁺ and Cd²⁺ from aqueous solution using chars from pyrolysis and microwave-assisted hydrothermal carbonization of *Prosopis africana* shell. *J. Ind. Eng. Chem.* **2014**, *20*, 3467–3473. [[CrossRef](#)]
13. Mohan, D.; Sarswat, A.; Ok, Y.S.; Pittman, C.U., Jr. Organic and inorganic contaminants removal from water with biochar, a renewable, low cost and sustainable adsorbent—A critical review. *Bioresour. Technol.* **2014**, *160*, 191–202. [[CrossRef](#)] [[PubMed](#)]
14. Beesley, L.; Inneh, O.S.; Norton, G.J.; Moreno-Jimenez, E.; Pardo, T.; Clemente, R.; Dawson, J.J.C. Assessing the influence of compost and biochar amendments on the mobility and toxicity of metals and arsenic in a naturally contaminated mine soil. *Environ. Pollut.* **2014**, *186*, 195–202. [[CrossRef](#)] [[PubMed](#)]
15. Houben, D.; Evrard, L.; Sonnet, P. Mobility, bioavailability and pH-dependent leaching of cadmium, zinc and lead in a contaminated soil amended with biochar. *Chemosphere* **2013**, *92*, 1450–1457. [[CrossRef](#)] [[PubMed](#)]
16. Uchimiya, M.; Bannon, D.I.; Wartelle, L.H. Retention of Heavy Metals by Carboxyl Functional Groups of Biochars in Small Arms Range Soil. *J. Agric. Food Chem.* **2012**, *60*, 1798–1809. [[CrossRef](#)] [[PubMed](#)]
17. Kołodyńska, D.; Wnętrzak, R.; Leahy, J.J.; Hayes, M.H.B.; Kwapiński, W.; Hubicki, Z. Kinetic and adsorptive characterization of biochar in metal ions removal. *Chem. Eng. J.* **2012**, *197*, 295–305. [[CrossRef](#)]
18. Zhou, Y.-F.; Haynes, R.J. Sorption of Heavy Metals by Inorganic and Organic Components of Solid Wastes: Significance to Use of Wastes as Low-Cost Adsorbents and Immobilizing Agents. *Crit. Rev. Environ. Sci. Technol.* **2010**, *40*, 909–977. [[CrossRef](#)]
19. Bulut, Y.; Baysal, Z. Removal of Pb(II) from wastewater using wheat bran. *J. Environ. Manag.* **2006**, *78*, 107–113. [[CrossRef](#)] [[PubMed](#)]
20. Bigham, J.; Nordstrom, D.K. Iron and aluminum hydroxysulfates from acid sulfate waters. *Rev. Miner. Geochem.* **2000**, *40*, 351–403. [[CrossRef](#)]
21. Simpson, S.; Vardanega, C.R.; Jarolimek, C.; Jolley, D.F.; Angel, B.M.; Mosley, L.M. Metal speciation and potential bioavailability changes during discharge and neutralisation of acidic drainage water. *Chemosphere* **2014**, *103*, 172–180. [[CrossRef](#)] [[PubMed](#)]
22. Creeper, N.L.; Shand, P.; Hicks, W.; Fitzpatrick, R.W. Porewater Geochemistry of Inland Acid Sulfate Soils with Sulfuric Horizons Following Postdrought Reflooding with Freshwater. *J. Environ. Qual.* **2015**, *44*, 989–1000. [[CrossRef](#)] [[PubMed](#)]
23. Creeper, N.L.; Hicks, W.S.; Shand, P.; Fitzpatrick, R.W. Geochemical processes following freshwater reflooding of acidified inland acid sulfate soils: An in situ mesocosm experiment. *Chem. Geol.* **2015**, *411*, 200–214. [[CrossRef](#)]
24. Mosley, L.; Palmer, D.; Leyden, E.; Cook, F.; Zammit, B.; Shand, P.; Baker, A.; Fitzpatrick, R.W. Acidification of floodplains due to river level decline during drought. *J. Contam. Hydrol.* **2014**, *161*, 10–23. [[CrossRef](#)] [[PubMed](#)]
25. Santos, I.R.; Eyre, B.D. Radon tracing of groundwater discharge into an Australian estuary surrounded by coastal acid sulphate soils. *J. Hydrol.* **2011**, *396*, 246–257. [[CrossRef](#)]
26. Mosley, L.; Fitzpatrick, R.; Palmer, D.; Leyden, E.; Shand, P. Changes in acidity and metal geochemistry in soils, groundwater, drain and river water in the Lower Murray River after a severe drought. *Sci. Total Environ.* **2014**, *485–486*, 281–291. [[CrossRef](#)] [[PubMed](#)]
27. Johnston, S.G.; Keene, A.F.; Bush, R.T.; Burton, E.D.; Sullivan, L.A.; Isaacson, L.; McElnea, A.E.; Ahern, C.R.; Smith, C.D.; Powell, B. Iron geochemical zonation in a tidally inundated acid sulfate soil wetland. *Chem. Geol.* **2011**, *280*, 257–270. [[CrossRef](#)]

28. Fitzpatrick, R.W.; Mosley, L.M.; Raven, M.D.; Shand, P. Schwertmannite formation and properties in acidic drain environments following exposure and oxidation of acid sulfate soils in irrigation areas during extreme drought. *Geoderma* **2017**, *308* (Suppl. C), 235–251. [[CrossRef](#)]
29. Krstic, D.; Djalovic, I.; Nikezic, D.; Bjelic, D. Aluminium in Acid Soils: Chemistry, Toxicity and Impact on Maize Plants. In *Plants, Food Production—Approaches, Challenges and Tasks*; Aladjadjian, A., Ed.; InTech: Rijeka, Croatia, 2012.
30. Hicks, W.S.; Bowman, G.M.; Fitzpatrick, R.W. Effect of season and landscape position on the aluminium geochemistry of tropical acid sulfate soil leachate. *Soil Res.* **2009**, *47*, 137–153. [[CrossRef](#)]
31. Rayment, G.E.; Lyons, D.J. *Soil Chemical Methods—Australia*; CSIRO Publishing: Victoria, Australia, 2011; Volume 3.
32. Aitken, R.; Moody, P. The effect of valence and Ionic-strength on the measurement of pH buffer capacity. *Soil Res.* **1994**, *32*, 975–984. [[CrossRef](#)]
33. Weber, T.; Allard, T.; Tipping, E.; Benedetti, M.F. Modeling Iron Binding to Organic Matter. *Environ. Sci. Technol.* **2006**, *40*, 7488–7493. [[CrossRef](#)] [[PubMed](#)]
34. Ahern, C.R.; McElnea, A.E.; Sullivan, L.A. Acid neutralising capacity, carbonate and alkali cation methods. In *Acid Sulfate Soils Laboratory Methods Guidelines*; Ahern, C.R., McElnea, A.E., Sullivan, L.A., Eds.; Department of Natural Resources, Mines and Energy: Indooroopilly, Australia, 2004.
35. Brunauer, S.; Emmett, P.H.; Teller, E. Adsorption of gases in multimolecular layers. *J. Am. Chem. Soc.* **1938**, *60*, 309–319. [[CrossRef](#)]
36. Zarcinas, B.A.; McLaughlin, M.J.; Smart, M.K. The effect of acid digestion technique on the performance of nebulization systems used in inductively coupled plasma spectrometry. *Commun. Soil Sci. Plant Anal.* **1996**, *27*, 1331–1354. [[CrossRef](#)]
37. McBeath, A.V.; Smernik, R.J.; Krull, E.S.; Lehmann, J. The influence of feedstock and production temperature on biochar carbon chemistry: A solid-state ¹³C NMR study. *Biomass Bioenergy* **2014**, *60*, 121–129. [[CrossRef](#)]
38. Zhang, J.; Lü, F.; Luo, C.; Shao, L.; He, P. Humification characterization of biochar and its potential as a composting amendment. *J. Environ. Sci.* **2014**, *26*, 390–397. [[CrossRef](#)]
39. Milne, C.J.; Kinniburgh, D.G.; de Wit, J.C.M.; van Riemsdijk, W.H.; Koopal, L.K. Analysis of proton binding by a peat humic acid using a simple electrostatic model. *Geochim. Cosmochim. Acta* **1995**, *59*, 1101–1112. [[CrossRef](#)]
40. Montenegro, A.C.; Orsetti, S.; Molina, F.V. Modelling proton and metal binding to humic substances with the NICA–EPN model. *Environ. Chem.* **2014**, *11*, 318–332. [[CrossRef](#)]
41. Bhatnagar, A.; Sillanpää, M. Utilization of agro-industrial and municipal waste materials as potential adsorbents for water treatment—A review. *Chem. Eng. J.* **2010**, *157*, 277–296. [[CrossRef](#)]
42. Kinniburgh, D.G.; Milne, C.J.; Benedetti, M.F.; Pinheiro, J.P.; Filius, J.; Koopal, L.K.; Van Riemsdijk, W.H. Metal Ion Binding by Humic Acid: Application of the NICA–Donnan Model. *Environ. Sci. Technol.* **1996**, *30*, 1687–1698. [[CrossRef](#)]
43. Kirby, C.S.; Cravotta Iii, C.A. Net alkalinity and net acidity 1: Theoretical considerations. *Appl. Geochem.* **2005**, *20*, 1920–1940. [[CrossRef](#)]
44. Mosley, L.; Willson, P.; Hamilton, B.; Butler, G.; Seaman, R. The capacity of biochar made from common reeds to neutralise pH and remove dissolved metals in acid drainage. *Environ. Sci. Pollut. Res.* **2015**, *22*, 15113–15122. [[CrossRef](#)] [[PubMed](#)]
45. Qian, L.; Chen, B. Interactions of Aluminum with Biochars and Oxidized Biochars: Implications for the Biochar Aging Process. *J. Agric. Food Chem.* **2013**, *62*, 373–380. [[CrossRef](#)] [[PubMed](#)]

